FSAR 1978
Food Science of Animal Resources
Food Sci. Anim. Resour. 2024 September 44(5):1108~1125
DOI https://doi.org/10.5851/kosfa.2024.e46
pISSN : 2636-0772 eISSN : 2636-0780
http://www.kosfaj.org

ARTICLE

Comparison of Soy and Pea Protein for Cultured Meat Scaffolds: Evaluating Gelation, Physical Properties, and Cell Adhesion

Do Hyun Kim†, Seo Gu Han†, Su Jin Lim, Seong Joon Hong, Hyuk Cheol Kwon, Hyun Su Jung, and Sung Gu Han*

Department of Food Science and Biotechnology of Animal Resources, Konkuk University, Seoul 05029, Korea

OPEN ACCESS

Received February 27, 2024
Revised April 8, 2024
Accepted June 10, 2024

***Corresponding author** : Sung Gu Han
Department of Food Science and Biotechnology of Animal Resources, Konkuk University, Seoul 05029, Korea
Tel: +82-2-450-0526
Fax: +82-2-4556-1044
E-mail: hansg@konkuk.ac.kr

***ORCID**
Do Hyun Kim
https://orcid.org/0000-0002-2500-8688
Seo Gu Han
https://orcid.org/0000-0001-5100-7446
Su Jin Lim
https://orcid.org/0000-0002-7646-013X
Seong Joon Hong
https://orcid.org/0009-0008-1410-3752
Hyuk Cheol Kwon
https://orcid.org/0000-0001-6234-2530
Hyun Su Jung
https://orcid.org/0000-0002-3491-8317
Sung Gu Han
https://orcid.org/0000-0002-1485-861X

† These authors contributed equally to this work.

Abstract Cultured meat is under investigation as an environmentally sustainable substitute for conventional animal-derived meat. Employing a scaffolding technique is one approach to developing cultured meat products. The objective of this research was to compare soy and pea protein in the production of hydrogel scaffolds intended for cultured meat. We examined the gelation process, physical characteristics, and the ability of scaffolds to facilitate cell adhesion using mesenchymal stem cells derived from porcine adipose tissue (ADSCs). The combination of soy and pea proteins with agarose and agar powders was found to generate solid hydrogels with a porous structure. Soy protein-based scaffolds exhibited a higher water absorption rate, whereas scaffolds containing agarose had a higher compressive strength. Based on Fourier transform infrared spectroscopy analysis, the number of hydrophobic interactions increased between proteins and polysaccharides in the scaffolds containing pea proteins. All scaffolds were nontoxic toward ADSCs, and soy protein-based scaffolds displayed higher cell adhesion and proliferation properties. Overall, the soy protein-agarose scaffold was found to be optimal for cultured meat production.

Keywords cultured meat, scaffold, stem cell, soy protein, pea protein

Introduction

As the global population grows, meat consumption is also increasing gradually. However, increasing livestock production capacity to meet this demand causes various problems such as animal welfare, environmental pollution, and abusing of antibiotics (Bhat and Fayaz, 2011; Tiberius et al., 2019). Cultured meat, also called cell-based meat, cultivated meat, or *in vitro* meat, is considered an alternative to conventional meat due to its potential to reduce the need for animal slaughter, lower the risk of animal disease and epidemics, and minimize water and land use (Hong et al., 2021; Zhang et al., 2020). Cultured meat is produced by growing adipose tissue derived-

mesenchymal stem cells (ADSCs), induced pluripotent stem cells, or other cells *in vitro* rather than raising and slaughtering animals (Datar and Betti, 2010; Jairath et al., 2021; Takahashi and Yamanaka, 2006). Several sheets of monocytes, 3D printing, and scaffolding methods have been used to develop 3D cultured meat products (Benjaminson et al., 2002; Datar and Betti, 2010).

Scaffolds are 3D porous structures that function as templates for tissue formation (O'brien, 2011). Scaffolds provide physical and biochemical cues for cells to adhere, proliferate, and differentiate into the necessary cell types, leading to a final product with a meat-like texture and structure that closely resembles conventional meat (Seah et al., 2022; Specht et al., 2018; Stephens et al., 2018). To be suitable for use as cultured meat technology, scaffolds must possess the following characteristics: edibility, sustainability, biocompatibility, animal-free composition, porosity, and biodegradability (Chen et al., 2022; O'brien, 2011). To meet these requirements, current studies are focused on investigating scaffolds made from hydrogels. Hydrogels possess a structure that is comparable to extracellular matrix (ECM), which enables high water retention potential, high porosity, and the potential presence of cell-adhesion ligands (Mobaraki et al., 2020). Despite their benefits, hydrogels have inherent limitations, such as restricted diffusion of nutrients and gases, and limited mechanical strength and rigidity when employed as scaffolds (Lee et al., 2019; Levato et al., 2020). Modifying the temperature, pressure, and component concentration, or freeze-drying can address these limitations and enhance the performance of hydrogel scaffolds (Seah et al., 2022). The freeze-dried hydrogel has a sponge-like shape and enhanced porous structure, making it an ideal scaffold for cultured meat with improved mechanical strength and rigidity (Las Heras et al., 2020; Xiang et al., 2022).

Plant proteins, such as soy, pea, and zein proteins are used in the production of cultured meat due to their affordability, edibility, biocompatibility, low cost, and ease of processing (Pan et al., 2022; Zhu et al., 2021). Plant proteins exhibit lower immunogenicity and higher polarity, rendering them naturally hydrophilic and potentially effective at promoting cell adhesion (Jahangirian et al., 2019; Reddy et al., 2011). Owing to these advantages, the development of biomaterials for tissue engineering, such as porous scaffolds and hydrogels, using plant-derived proteins has increased (Lin et al., 2016; Tansaz et al., 2018). However, scaffolds made from plant proteins typically lack physicochemical and biological properties for cultured meat (Jahangirian et al., 2019). To address this issue, synthetic polymers were often mixed with proteins to improve their mechanical strength, resistance to water, compatibility with living tissues, and overall suitability (Jahangirian et al., 2019).

Polysaccharides, such as agarose, agar, carrageenan, and guar gum, are extensively utilized as food additives and can form a stable 3D structure due to their gelation ability (Bektas et al., 2021). However, polysaccharides have limited capacity for cell adhesion without chemical or physical modifications (Bektas et al., 2021; Yixue et al., 2013). Since proteins can provide cell adhesion motif, crosslinking of proteins and polysaccharides enables the production of scaffolds with both high cell adhesion and stable physical properties (Ben-Arye et al., 2020). For example, a polysaccharide, konjac glucomannan, had positive effect on the hardness, chewiness, gel strength, and compact gel structure in plant-based fish balls made with soy protein isolate and konjac glucomannan (Ran et al., 2022).

Limited information is available on the development of plant protein and polysaccharide-based scaffolds for cultured meat. Thus, the aim of this study was to evaluate and compare the gelation, physical properties, cytotoxicity, and cell adhesion capacity of porcine ADSCs isolated from Berkshire pigs using scaffolds composed of soy and pea proteins, as well as agarose and agar.

Materials and Methods

Preparation of scaffolds

Two polysaccharides, agarose (Fisher BioReagents, Pittsburgh, PA, USA) and agar powder (Duksan Pure Chemicals,

Ansan, Korea); and two protein isolates, pea protein (Emsland-Starke, Emlichheim, Germany) and soy protein (Shandong Yuxin Bio-Tech, Shangdong, China), were used to prepare the hydrogel scaffolds. The protein contents of isolated soy and pea proteins were 90% and 85%, respectively. The formulations of the protein-polysaccharide hydrogels and scaffolds are listed in Table 1. Soy and pea protein solutions were prepared as described in previous studies, with slight modifications (Yan et al., 2020; Zhu et al., 2021). Protein isolates were dissolved in distilled water at different concentrations (0%, 2.5%, 5%, or 10%, w/v) and stirred at room temperature for 3 h. Thereafter, the soy protein was heated in a water bath at 90°C for 30 min and cooled to 25°C for 30 min with cold water. After the pH was adjusted to 7 using 1 mol/L HCl, the total volume was adjusted to 100 mL and stored at 37°C until use. After the pea protein was stirred, the pH was adjusted to 12 using 1 mol/L NaOH and the mixture was stirred at room temperature for 1 h. The pea protein was then heated in a water bath at 80°C for 10 min and cooled in cold water for 10 min. After the pH of the pea protein solution was adjusted to 7 using 1 mol/L HCl, the total volume was adjusted to 300 mL and stored at 37°C until use.

Both polysaccharide solutions were prepared under the same conditions and dissolved in distilled water at a concentration of 2% w/v in a microwave (Wollschlaeger et al., 2022). The solutions were then combined in a 1:1 ratio with a pre-warmed mixture of pea protein isolates and soy protein isolate solutions in different stock solutions (0%, 2.5%, 5%, or 10% w/v). Subsequently, 500 μL of the warm hydrogel solution was transferred into each well of a 48-well plate (SPL Life Sciences, Pocheon, Korea) and allowed to cool to room temperature for 15 min for hydrogel. The final protein concentrations of the hydrogels were 0%, 1.25%, 2.5%, and 5%, and the final polysaccharide concentration was 1%. The hydrogels were stored overnight at –20°C, and then overnight at –80°C. Finally, the hydrogels were freeze-dried for 3 days.

Fourier transform infrared spectroscopy

The bonding transition of the hydrogels was analyzed using an fourier transform infrared (FT-IR) spectrophotometer (FT/IR-4700, JASCO, Tokyo, Japan), according to a previously described methodology (Cesur et al., 2020). Spectral data were obtained over the range of 500−4,000 cm^{-1} at a resolution of 1 cm^{-1}. The hydrogels were prepared in 48-well plates and analyzed in triplicate.

Scanning electron microscopy

Scanning electron microscopy (SEM; JSM-6380, JEOL, Tokyo, Japan) was used to investigate the porous morphologies of the scaffolds. To assess the porous structure both internally and externally within the scaffolds, images were captured from both the top and cross-sectional portions of the scaffold. The scaffold samples were fixed on the SEM support and sputtered with platinum (Sputter Coater 180, Cressington Scientific Instruments, Watford, UK). Finally, the morphologies of the scaffolds were recorded.

Table 1. Formulation of the protein-polysaccharide hydrogels and scaffolds

Hydrogels/scaffolds	Soy protein isolate (2.5%)	Pea protein isolate (2.5%)	Agarose (1%)	Agar powder (1%)
SA	+	–	+	–
SAP	+	–	–	+
PA	–	+	+	–
PAP	–	+	–	+

SA, soy protein-agarose hydrogel; SAP, soy protein-agar powder hydrogel; PA, pea protein-agarose hydrogel; PAP, pea protein-agar powder hydrogel; +, the scaffold incorporates this material; –, this material is not incorporated into the scaffold.

Water absorption test

To evaluate the water absorption properties of the scaffolds, the scaffolds were first weighed to obtain their dry weights (W_d). Thereafter, the scaffolds were immersed in phosphate-buffered saline (PBS) at room temperature for 1, 3, 5, and 7 days. After each immersion period, the excess surface moisture was removed using Kimtech (Yuhan Kimberly, Seoul, Korea). The scaffolds were then weighed to obtain their wet weight (W_w). The water absorption (%) of each scaffold was calculated using the following Eq. (1):

$$\text{Water absorption (\%)} = (W_w - W_d / W_d) \times 100 \quad (1)$$

Compressive stress test

The mechanical properties of the scaffolds were analyzed using a texture analyzer (TA-XT Plus, Stable Micro Systems, Goldaming, UK) via unconfined compression tests. The scaffolds, which had a diameter of 9 mm and height of 7 mm, were positioned between parallel plates made of stainless steel. The stress response and elastic recovery were recorded while the scaffolds were subjected to 60% strain at a rate of 1.0 mm/s. The stress/strain curves were generated using the Exponent Connect software.

Isolation of adipose derived stem cells

ADSCs were isolated from the back fat of 12 months old Berkshire piglet. The resected tissues were rinsed and soaked in sterile PBS supplemented with 10% antibiotic-antimycotic (AA; Gibco™, New York, NY, USA). Fat tissues were separated from muscle tissues using sterile tweezer/scissors in PBS with 10% AA. For digestion, fat tissues were transferred to a sterile 50 mL conical tube and centrifuged at 2,000×g (MF80; Hanil Science Industrial, Incheon, Korea) for 5 min. The supernatants were discarded, and the residual fat tissues were digested using a 0.2% digestion solution consisting of 100 mg collagenase type 2, 5 mL of 10% AA, and 45 mL of PBS. The digestion was allowed to proceed in a shaking incubator at 37°C for 1 h. After incubation, the cells were filtered and centrifuged at 2,500×g for 5 min. The supernatants were discarded, and the cells were incubated with ammonium-chloride-potassium lysis buffer (Gibco™) at 4°C for 5 min. Thereafter, 5 mL of neutralization medium was added, and the mixture was centrifuged at 1,000×g for 5 min. The isolated cells were resuspended with minimum essential media alpha (MEM α, Gibco™) supplemented with 10% fetal bovine serum (FBS), 1% AA, and 10 ng/mL of basic fibroblast growth factor (Bio-Techne, Minneapolis, MN, USA). Finally, the cells were seeded in a new culture flask.

Cell culture

ADSCs (passage 4–8) were used for all experiments and were cultured in a humidified incubator at 37°C under 5% CO_2. The cells were maintained in MEM-α supplemented with 10% FBS (Welgene, Gyeongsan, Korea), 1% (v/v) penicillin/ streptomycin glutamine (Gibco™), and 10 ng/mL bFGF. Upon reaching approximately 80% confluence, the cells were trypsinized and passaged. The growth medium was also refreshed daily.

Indirect cytotoxicity test

An indirect cytotoxicity test was performed as previously described, with some modifications (Wollschlaeger et al., 2022). The scaffolds were sterilized via soaking in 70% ethanol overnight, exposed to UV light for 2 h (1 h per side), and then washed

three times with sterile PBS. The scaffolds were filled with growth medium at a scaffold-to-medium ratio of 1:4 (v/v) and placed in an incubator at 37°C and 5% CO_2 for 1 or 3 days to facilitate scaffold extraction. Growth medium was incubated under identical conditions and used as a control. Prior to testing, the cells were seeded in a 96-well plate (SPL Life Sciences) at a density of 2×10^4 cells/well. Once the cells reached approximately 80% confluency, the growth medium was replaced with 1- or 3-day scaffold extract or control medium. After 1 day of incubation, the cells were analyzed using a lactate dehydrogenase (LDH) activity assay and a 3-(4,5-dimethylthiazol-2yl)-2,5-diphenyl-2*H*-tetrazolium bromide (MTT) assay.

Lactate dehydrogenase activity assay

LDH assay was conducted to assess the cytotoxicity of the scaffolds using an LDH Cytotoxicity Assay Kit (Promega, Madison, WI, USA). Lysis buffer was added to the cells 45 min prior to the end of the 1-day incubation period to serve as the positive control (maximum LDH release). After the incubation period, 50 μL of supernatant from each well was transferred to a new 96-well plate and mixed with 50 μL of the LDH assay buffer. The plate was incubated in the dark at room temperature for 30 min. The OD was measured at 490 nm using an Epoch spectrophotometer (BioTek Instruments, Winooski, VT, USA) and the percentage of LDH release was calculated using the following Eq. (2):

$$\text{LDH release } (\%) = [(\text{OD}_{\text{sample LDH release}} / \text{OD}_{\text{maximum LDH release}}) \times 100]. \quad (2)$$

Cell viability assay

The viability of cells was measured using the MTT assay. After 1 day of incubation, the liquid extracts from days 1 and 3 and the control medium were removed. The cells were incubated with the MTT reagent (Amresco, Solon, OH, USA) for 3 h and then with acidic isopropanol to dissolve the deposited formazan. The OD was measured at 570 and 630 nm using an Epoch spectrophotometer (BioTek Instruments). To calculate the percentage cell viability, the OD at 630 nm was subtracted from that at 570 nm using the following formula:

$$\text{Cell viability } (\%) = (\text{OD}_{\text{sample}} / \text{OD}_{\text{control}}) \times 100 \quad (3)$$

Live/dead-staining

The cells were cultured in 24-well plates until approximately 80% confluency was achieved. The growth medium was then replaced with 1- of 3-day liquid extract or control medium. After 1 day of incubation, the cells were stained using a live/dead cell imaging kit (Life Technologies, Eugene, OR, USA), according to the manufacturer's instructions. Live and dead cells were visualized and captured using a Nikon Eclipse Ti2-U and Nikon Eclipse Ts2R cameras (Nikon, Tokyo, Japan), with excitation wavelengths of 488 nm (green, indicating live cells) and 570 nm (red, indicating dead cells).

Scaffold cell seeding process and media cell counting

The scaffolds were sterilized with 70% ethanol before cell seeding as described above. After sterilization, the scaffolds were soaked in medium for 1 h. The excess medium in the scaffold was removed via slight extrusion, and the scaffolds were seeded with 1×10^7 cells per scaffold. Cells were allowed to adhere to the scaffolds for 1 day. The growth medium was subsequently introduced into the scaffolds, with changes made twice daily.

To evaluate the adhesion efficiency of cells to the scaffolds, the number of non-adherent cells was quantified using the previously described method (Zheng et al., 2022). In brief, following 1 day of cell adhesion, the cell count in the medium was determined using a hemocytometer (Hausser Scientific, Horsham, PA, USA).

Cell proliferation test

On days 3 and 5 after seeding cells onto the scaffolds, the samples were washed twice with PBS, fixed with 4% paraformaldehyde, stained with 4′,6-diamidino-2-phenylindole (DAPI; 1 μg/mL) for 10 min, and washed three times with PBS. The nuclei (emitting blue fluorescence) were then visualized and captured using a Nikon Eclipse Ts2R camera (Nikon).

Field emission scanning electron microscope examination

On days 3 and 5 after cell seeding on the scaffolds, the samples were washed twice with sterile PBS, immersed in a 2.5% glutaraldehyde solution for 3 h, and dehydrated using graded concentrations of ethanol (50%, 60%, 70%, 80%, 90%, and 100%, v/v) for 15 min. After freeze-drying, the samples were fixed on the field emission scanning electron microscope (FE-SEM) support, sputtered with platinum (Sputter Coater 180, Cressington Scientific Instruments) under vacuum, and examined using FE-SEM (SU-8010, Hitachi, Tokyo, Japan).

Statistical analysis

The data are presented as mean±standard error of mean. Statistical analyses were conducted using SPSS-PASW statistics software (version 18.0, SPSS, Chicago, IL, USA) with one-way analysis of variance (ANOVA). Tukey's post-hoc test ($p<0.05$) was performed to assess differences among the treatment means.

Results

The formation of protein-polysaccharide hydrogels and lyophilized scaffolds

Soy and pea proteins combined with agarose and agar powder resulted in the formation of solid hydrogels. As shown in Fig. 1A, the hydrogel mixture was poured into a beaker and allowed to solidify. Even when flipped, the resulting hydrogel remained in the solid state without flowing out. Lyophilizing these protein-polysaccharide hydrogels could produce solid scaffolds while preserving their form and structural integrity (Fig. 1B).

Effect of protein concentration on the properties of the protein-polysaccharide hydrogel and scaffolds

The influence of protein concentration on the properties of the protein-polysaccharide hydrogels and scaffolds is shown in Fig. 2. As the soy and pea protein concentrations increased, the hydrogels became firmer and exhibited greater solidity than the hydrogel containing 0% protein (Fig. 2A). Interestingly, despite variations in the type of polysaccharide used, increasing the protein concentration resulted in a significant increase in hydrogel solidity and yellow color in all groups, each composed of 1% polysaccharides. The 2.5% soy and pea proteins exhibited optimal hydrogel and freeze-dried scaffold characteristics, effectively maintaining shape and size (Figs. 2A and B). Conversely, the 5% protein hydrogel did not achieve uniformity due to rapid gelling. Consequently, the combination of 2.5% soy and pea proteins with 1% polysaccharides emerged as the most optimal choice for producing hydrogel and freeze-dried scaffold.

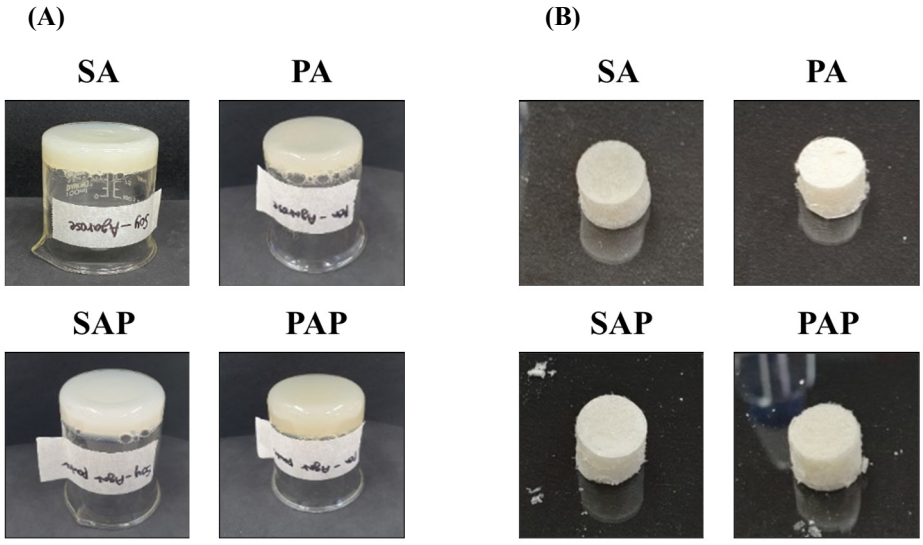

Fig. 1. Formation of hydrogel and lyophilized scaffolds using the mixture of protein and polysaccharide solution. (A) Formation of hydrogel by mixing 2.5% proteins (soy or pea) and 1% polysaccharides (agarose or agar powder). (B) Production of scaffolds by lyophilizing the hydrogels. The warm hydrogel solutions were cooled and lyophilized in a 48-well plate. SA, soy protein-agarose hydrogel; SAP, soy protein-agar powder hydrogel; PA, pea protein-agarose hydrogel; PAP, pea protein-agar powder hydrogel.

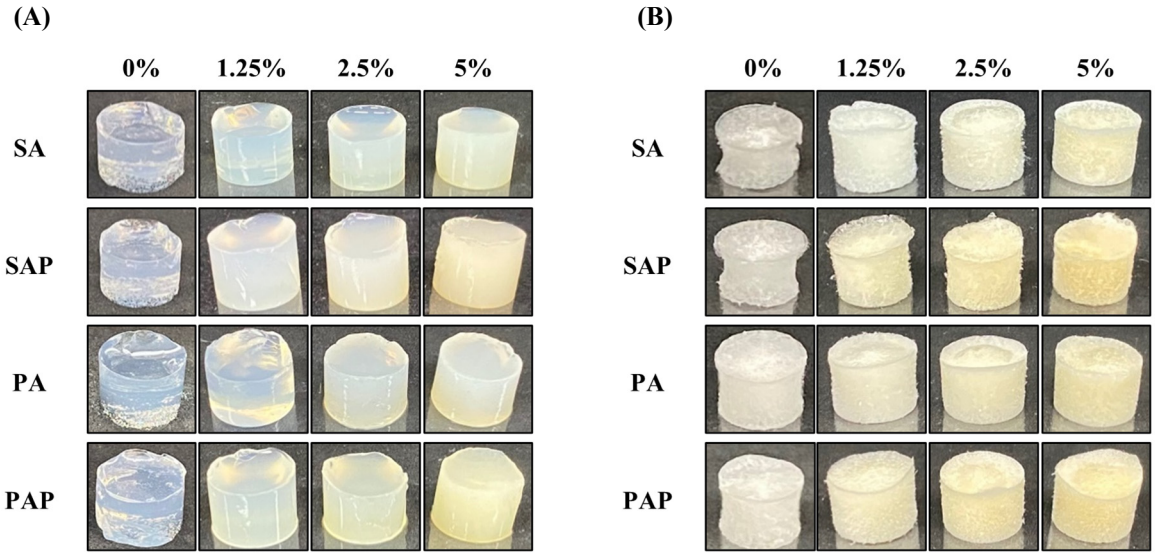

Fig. 2. Hydrogel and scaffold formation with different concentrations of protein solutions. (A) Hydrogel formation of protein-polysaccharide solution mixed with 0%, 1.25%, 2.5%, and 5% soy and pea proteins and 1% agarose and agar powder. (B) Scaffold formation of protein-polysaccharide hydrogels mixed with 0%, 1.25%, 2.5%, and 5% soy and pea proteins and 1% agarose and agar powder. SA, soy protein-agarose hydrogel; SAP, soy protein-agar powder hydrogel; PA, pea protein-agarose hydrogel; PAP, pea protein-agar powder hydrogel.

Structural properties of the protein-polysaccharide hydrogels

The structure of the protein-polysaccharide hydrogel was analyzed using FT-IR spectroscopy. Fig. 3 shows the peaks resulting from the chemical interactions between the proteins and polysaccharides. All protein-polysaccharide hydrogels exhibited the same peaks at 3,000–3,600 cm^{-1} and 1,633 cm^{-1}, which correspond to hydrogen bonds and protein peptides, respectively (Garrido et al., 2016; Jackson and Mantsch, 1992). Moreover, hydrogels containing pea protein [pea protein-agarose hydrogel (PA) and pea protein-agar powder hydrogel (PAP)] displayed slightly higher peaks at 2,986 cm^{-1} and 1,073

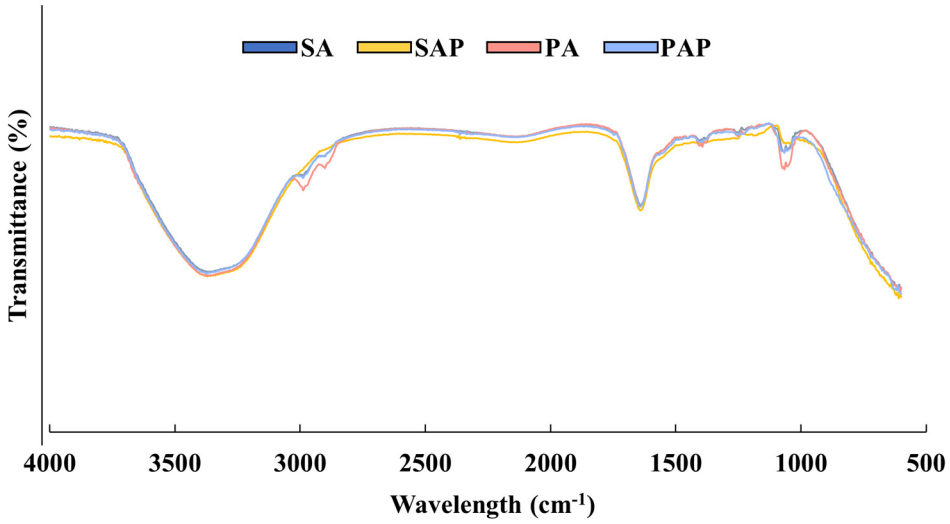

Fig. 3. Fourier-transform infrared (FT-IR) spectra of the protein-polysaccharide hydrogels. Protein-polysaccharide hydrogels were prepared by mixing 2.5% proteins (soy and pea) and 1% polysaccharides (agarose and agar powder). The peaks detected at 3,300 cm^{-1} indicate O-H stretching, whereas those detected at 2,969 cm^{-1} indicate C-H_2 stretching. The peaks detected at 1,633 cm^{-1} indicate C=O stretching and those at 1,073 cm^{-1} indicate C-O stretching vibrations (n=3). SA, soy protein-agarose hydrogel; SAP, soy protein-agar powder hydrogel; PA, pea protein-agarose hydrogel; PAP, pea protein-agar powder hydrogel.

cm^{-1} than soy protein hydrogels [soy protein-agarose hydrogel (SA) and soy protein-agar powder hydrogel (SAP); Fig. 3]. The intensities of the absorption band at 2,986 cm^{-1} and 1,073 cm^{-1} indicates C-H_2 and C-O stretching vibrations, respectively (de Oliveira et al., 2019; Hu et al., 2019). Based on our results, the protein-polysaccharide hydrogel has a stable structure owing to chemical interactions, such as hydrogen bonds and non-covalent interactions.

Physical characterization of the plant-based hydrogel scaffolds

Fig. 4A shows the water absorption rates of the scaffolds, which were measured on days 1, 3, 5, and 7. The water absorption ability of the scaffolds remained unchanged even with increasing treatment time. Scaffolds containing soy protein (SA and SAP) exhibited water absorption rates ranging from 2,300% to 2,500% on days 1, 3, 5, and 7, whereas scaffolds containing pea protein (PA and PAP) had significantly lower water absorption rates ranging from 1,100% to 1,200%. No significant difference was found between groups treated with the same protein, regardless of the polysaccharide used ($p>0.05$). However, a significant difference was observed between the different types of plant-based proteins ($p<0.05$). The water absorption rate data suggest that the physical properties of the protein-polysaccharide scaffolds remained stable even after prolonged exposure to the culture medium.

The different polysaccharides exhibited varying compressive strengths in the scaffolds (Fig. 4B). The agarose-based scaffolds (SA and PA) exhibited higher compressive strengths than those fabricated using agar powder (SAP and PAP). No differences in compressive strength were observed among the different proteins. Based on the compressive test, the scaffold prepared using agarose possessed more rigid properties than that prepared using agar powder.

The microstructures of the scaffolds are shown in Fig. 4C. The use of different protein-polysaccharide complexes resulted in varying porous microstructures in the scaffolds. SEM was used to examine the microstructure of the scaffolds. A similar level of porosity was observed in the top and cross-sections of the scaffolds. This result suggests that the protein-polysaccharide scaffold has a porous structure, which is crucial for facilitating 3D cell culture in cultured meat production.

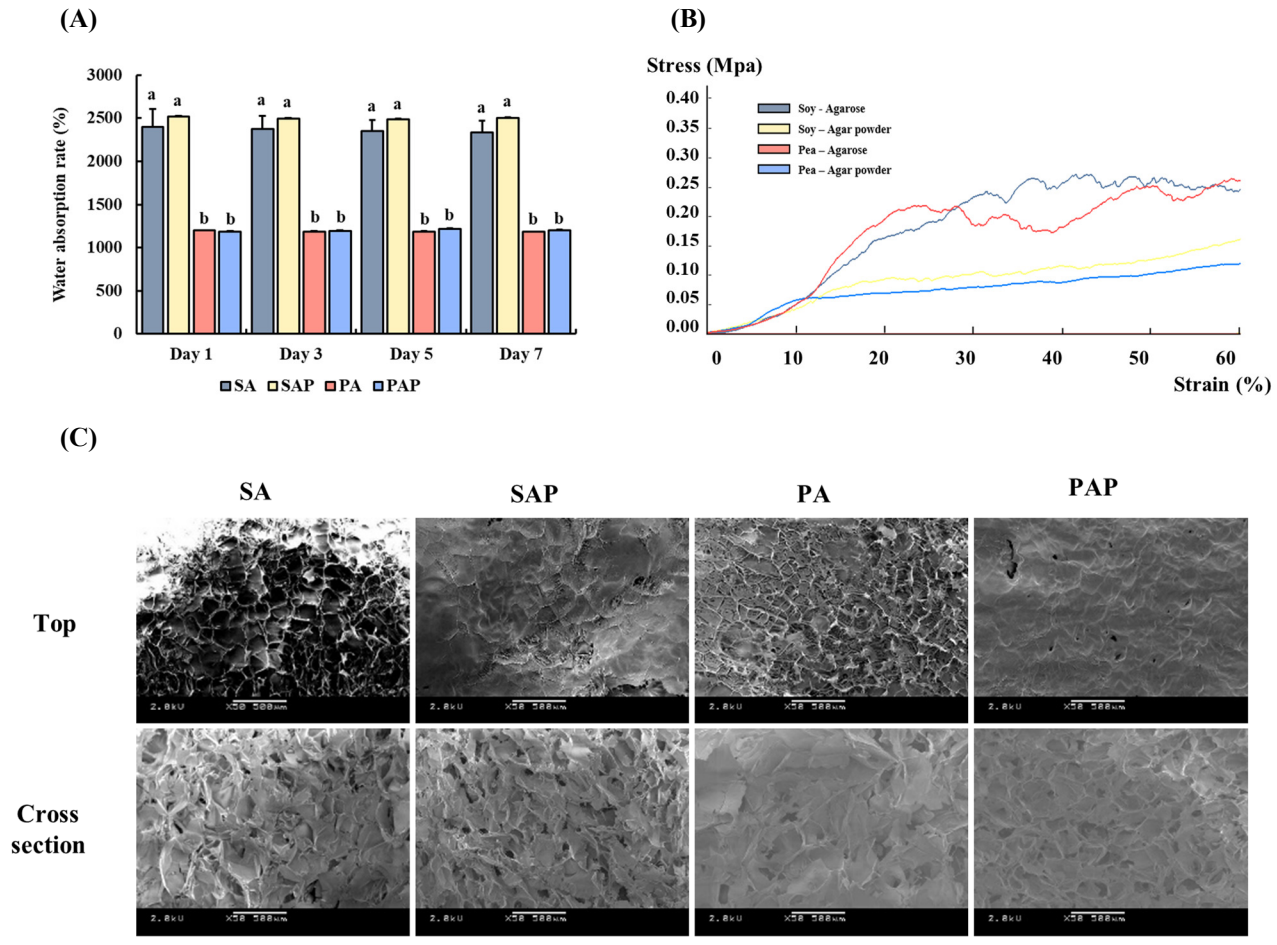

Fig. 4. Physical properties of the protein-polysaccharide scaffolds. (A) Water absorption properties of the protein-polysaccharide scaffolds. (B) Compressive strength of the protein-polysaccharide scaffolds. (C) Porous structure of protein-polysaccharide scaffold. Cross section and top surface were captured using scanning electron microscopy (white bar=500 μm). All experiments were repeated at least three times. The data are presented as mean±SD (n=4). ^{a,b} Different letters indicate a significant difference in the water absorption rate based on Tukey's post hoc test ($p<0.05$). SA, soy protein-agarose hydrogel; SAP, soy protein-agar powder hydrogel; PA, pea protein-agarose hydrogel; PAP, pea protein-agar powder hydrogel.

Impact of scaffold liquid extracts on cytotoxicity and cell viability

ADSCs were treated with liquid extracts from the scaffolds for 1 day and 3 days to determine their cytotoxicity. In the MTT and LDH assays, ADSCs treated with liquid extracts of SA, SAP, PA, or PAP on days 1 and 3 exhibited cell viability (Fig. 5A) and LDH release (Fig. 5B) similar to the control group ($p>0.05$). In addition, live/dead staining was performed to observe live ADSCs treated with the liquid extract of the scaffolds (Fig. 5C). On days 1 and 3, no significant differences were found between all groups and the control group, with a high ratio of green-stained live cells to few red-stained dead cells. Our results indicate that the scaffolds are not toxic and are suitable for use in food products.

Characterization of cell attachment and proliferation on scaffolds

The attachment and proliferation of ADSCs on the scaffolds were analyzed using FE-SEM imaging (Fig. 6A). The images depict ADSCs on the scaffolds after 3 and 5 days of inoculation. The cells were successfully attached to the SA and SAP surfaces on day 3. On day 5, the attached cells grew and proliferated, and maintained their spherical morphology. In contrast,

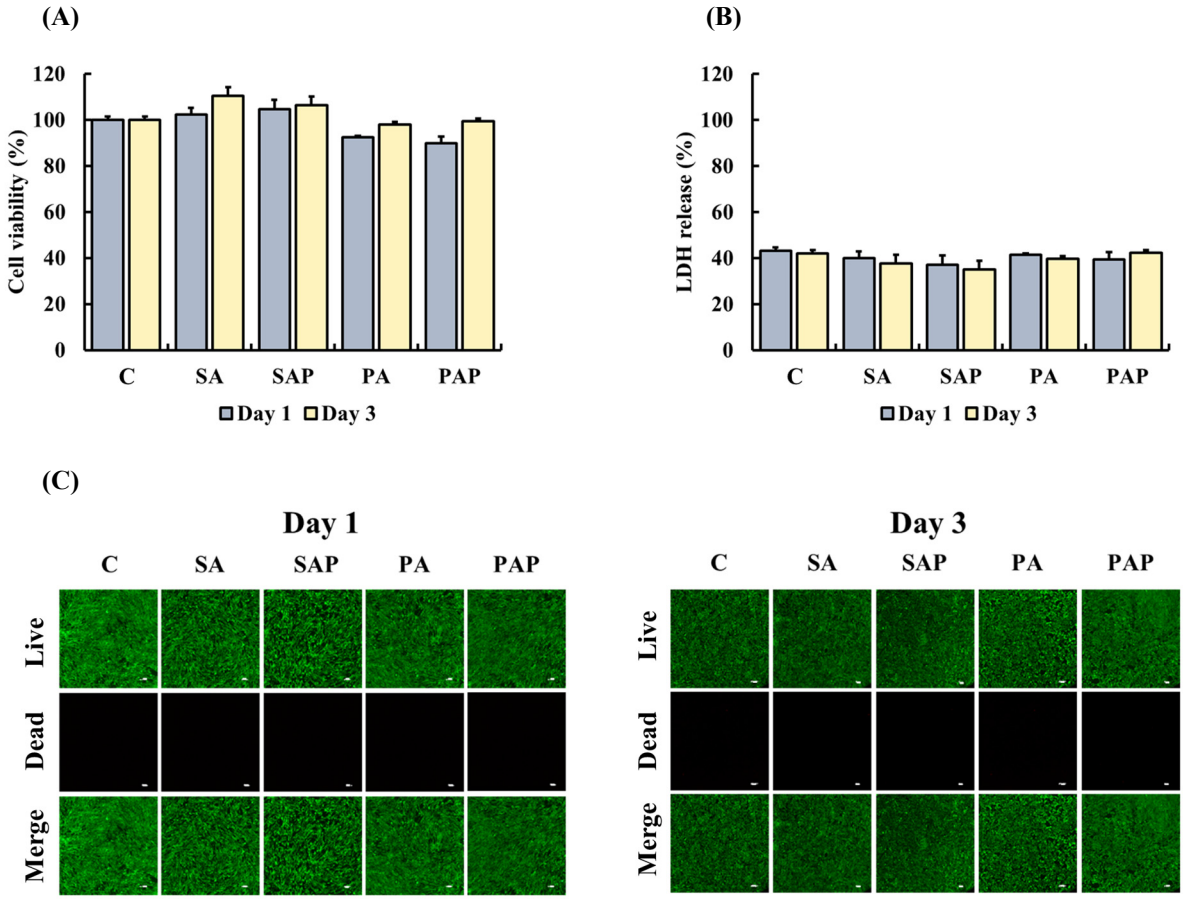

Fig. 5. Cytotoxicity of the protein-polysaccharide scaffolds. Adipose tissue-derived stem cells (ADSCs) from Berkshire piglet were treated with the liquid extract of scaffolds. Liquid extracts of scaffolds were prepared by incubating scaffolds with medium (scaffold-medium ratio 1:4) for 1 day. (A) Viability of ADSCs treated with the liquid extract of scaffolds. Cells were treated with the liquid extract of scaffolds for 1 day. (B) Lactate dehydrogenase (LDH) release of ADSCs treated with the liquid extract of scaffolds. Cells were treated with the liquid extract of scaffolds for 1 day. (C) Live/dead staining of ADSCs treated with the liquid extract of scaffolds. Cells were treated with the liquid extract of scaffolds for 1 day and 3 days. Scale bars: 100 μm. Green: viable cells; red: dead cells. All experiments were repeated at least three times. No significant differences in cell viability and LDH release were found based on Tukey's post hoc test ($p>0.05$). The data are presented as mean±SD (n=4). C, control; SA, soy protein-agarose hydrogel; SAP, soy protein-agar powder hydrogel; PA, pea protein-agarose hydrogel; PAP, pea protein-agar powder hydrogel.

PA and PAP exhibited limited cell attachment on day 3. Although some proliferation was observed on day 5, the degree was not as extensive as that in SA and SAP. Additionally, the number of detached cells in the medium was quantified 1 day after seeding (Fig. 6B). Among the scaffolds, SA resulted in the lowest cell count ($p<0.05$), suggesting that soy protein and agarose are optimal materials for enhancing cell adhesion properties. Furthermore, the proliferation of ADSCs on the scaffolds was evaluated using DAPI staining after 3 and 5 days of cell seeding (Fig. 6C). After 3 days, SA and SAP exhibited some cell attachment, whereas PA and PAP showed limited cell attachment. After 5 days of cell seeding, SA exhibited a higher number of proliferating cells, indicating better cell proliferation than SAP. However, PA and PAP exhibited cell numbers similar to those observed on day 3.

Discussion

In the present study, the gelation, chemical structure, and physical properties of plant protein-polysaccharide scaffolds

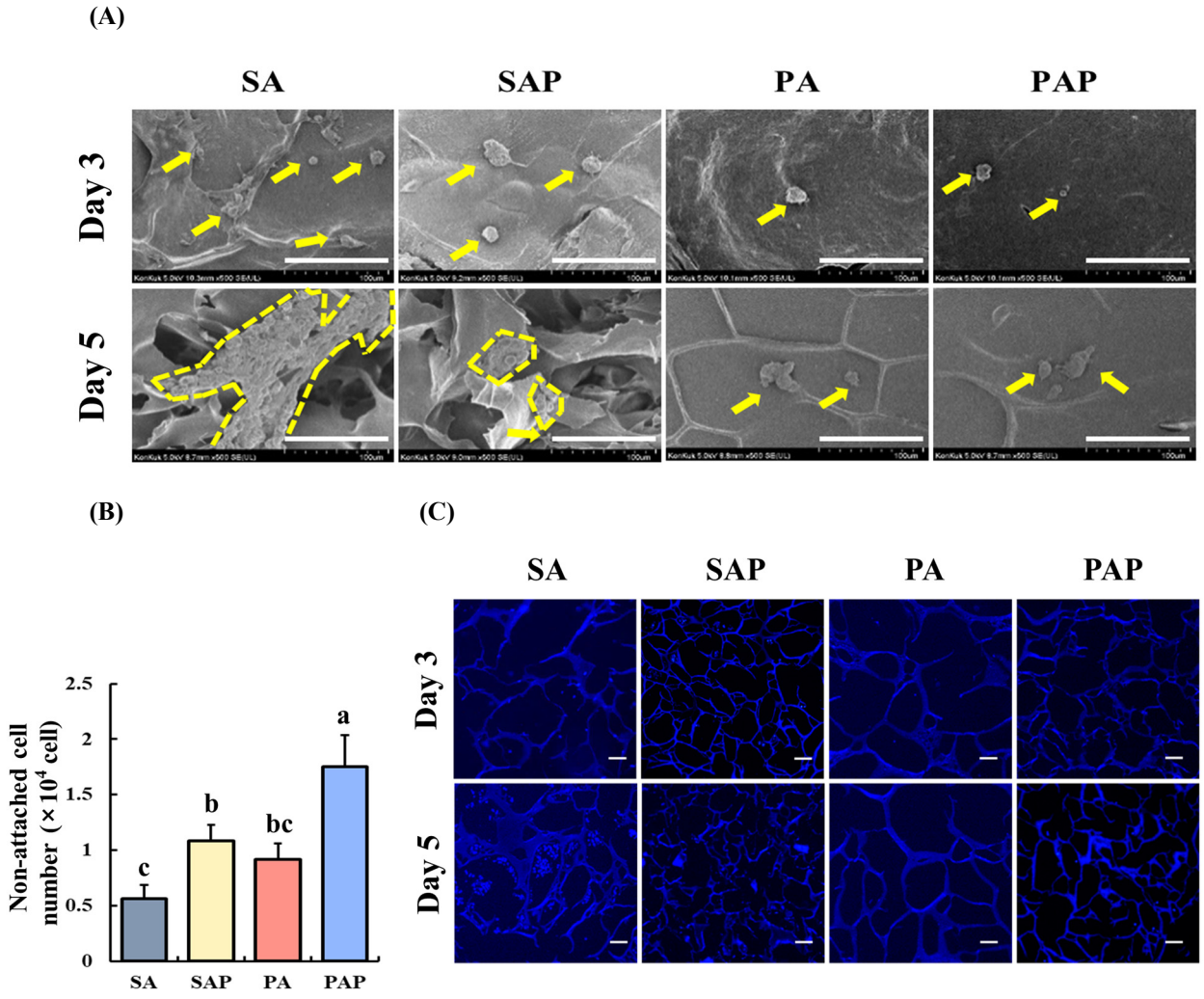

Fig. 6. Cell adhesion properties of the protein-polysaccharide scaffolds. (A) Adipose tissue-derived stem cells (ADSCs) on scaffolds captured based on field emission scanning electron microscope (FE-SEM, white bar=100 μm). A total of 1×10^7 of ADSCs were inoculated in scaffolds. At 3 and 5 days after inoculation, ADSCs were captured. Yellow arrow and dotted line indicate ADSCs. (B) The number of ADSCs that did not adhere to the scaffolds. At 1 day after ADSC inoculation, the number of cells in the growth medium was counted. (C) The nucleus (DAPI, white bar=100 μm) of ADSCs after 3 and 5 days of incubation. All experiments were repeated at least three times. $^{a-c}$ Different letters indicate a significant difference in the number of cells based on Tukey's post hoc test ($p<0.05$). The data are presented as mean±SD (n=4). SA, soy protein-agarose hydrogel; SAP, soy protein-agar powder hydrogel; PA, pea protein-agarose hydrogel; PAP, pea protein-agar powder hydrogel; DAPI, 4',6-diamidino-2-phenylindole.

were investigated. In addition, the adhesive and proliferative properties of ADSCs derived from Berkshires on the scaffolds were evaluated. We selected ADSCs due to their multi-directional differentiation potential which allows them to differentiate not only into adipocytes but also into muscle cells (Liu et al., 2022; Tsuji et al., 2014).

To make sustainable and cost-effective scaffolds, recent studies have investigated proteins and polysaccharides derived from plant or microbial sources. Pea and soy proteins, and agar/agarose have been employed as sources of proteins, stabilizers, and gelling agents in food additives (EFSA Panel on Food Additives and Nutrient Sources added to Food, 2016; Langyan et al., 2022). For instance, researchers evaluated hydrogels synthesized using a blend of plant-derived proteins (pea and soy proteins) and polysaccharides (agarose, gellan, and a xanthan-locust bean gum blend) to assess their potential use in cultured meat (Wollschlaeger et al., 2022). This previous research demonstrated that protein-polysaccharide gels remained

stable at lower protein concentrations (up to 1%), but not at higher concentrations. Additionally, the study revealed that none of the hydrogels displayed cytotoxic effects on immortalized myoblast cells. In another study, a scaffold developed using wheat glutenin was found to possess sufficient porous structure, water absorption capacity, mechanical strength, and the ability to promote C2C12 cell proliferation and differentiation, making it suitable for use in cultured meat production (Xiang et al., 2022).

Soy and pea proteins are ideal for hydrogel manufacturing owing to their excellent cohesion and gelation properties (Lam et al., 2018). Additionally, soy protein contains lunasin peptides that include an arginylglycylaspartic acid (RGD) motif, a cell-attachment region for extracellular substrates (Ben-Arye et al., 2020; Gonzalez de Mejia et al., 2010). Agarose is a natural linear polysaccharide that is primarily extracted from certain red seaweed (te Nijenhuis, 1997), while agar is a mixture of two polysaccharides: agarose and agaropectin (Armisén and Gaiatas, 2009). Both agarose and agar are commonly used in food products as gelling agents, gelatin substitutes, and stabilizers owing to their gelation properties and affordability (Lei et al., 2022). Therefore, we selected agarose and agar as our polysaccharide sources to improve the stability of the plant protein hydrogel.

In previous studies, protein solutions with concentrations higher than 5% were not found to form stable gels (Wollschlaeger et al., 2022). To increase protein solubility, we varied the pH and temperature as described previously with slight modifications. In particular, we mixed 0%, 2.5%, 5%, and 10% protein solutions with 2% polysaccharide solutions to obtain hydrogels with 0%, 1.25%, 2.5%, and 5% soy and pea protein concentrations. All protein solutions formed stable hydrogels, with higher protein concentrations resulting in more compact gels. However, during the titration process, 10% of the pea proteins gelled before reaching a pH of 12, resulting in the formation of less uniform gels. This result is due to the aggregation of protein molecules in highly concentrated solutions (Louche et al., 2017). Therefore, we identified 5% soy and pea protein solution as the optimal protein concentration for unified hydrogels.

The chemical interactions between the proteins and polysaccharides were investigated by analyzing their FT-IR spectra. The hydrogels exhibited significant peaks at 3,300 cm^{-1}, 2,986 cm^{-1}, 2,969 cm^{-1}, 1,633 cm^{-1}, and 1,073 cm^{-1}. All hydrogels showed the same intensity at 3,300 cm^{-1} and 1,633 cm^{-1}. The band at 1,633 cm^{-1} (amide I band) was assigned to the C=O stretching vibration of peptide linkages in the backbone of the protein (Jackson and Mantsch, 1992). The broad band observed in the 3,000–3,600 cm^{-1} range was related to the free and bound O-H and N-H groups, indicating the formation of hydrogen bonds between the hydroxyl groups of the protein and agarose (Garrido et al., 2016). Soy and pea protein isolates are composed of various amino acid residues that possess functional groups, such as carboxylic acids, amines, and hydroxyl groups. These functional groups can interact with agarose, which has a highly hydrated surface due to the abundance of hydroxyl groups (Amitai et al., 2004). Electrostatic interactions between the negatively charged carboxylate groups on soy proteins and the positively charged hydrogen atoms on agarose can lead to attractive forces between the two molecules (Sun, 2005). Hydrogen bonding can occur between the polar groups of soy protein isolates and agarose, such as amide and hydroxyl groups (Habermann and Murphy, 1996). These interactions can be attributed to the formation of a stable hydrogel. We observed distinct peaks at 2,986 cm^{-1}, 2,969 cm^{-1}, and 1,073 cm^{-1} for each hydrogel. Interestingly, hydrogels containing pea proteins (PA and PAP) displayed higher absorption band intensities than those containing soy proteins (SA and SAP) from the same polysaccharide source. The peaks at 2,969 cm^{-1} and 1,073 cm^{-1} are associated with the C-H_2 and C-O stretching vibrations, respectively (de Oliveira et al., 2019; Hu et al., 2019). These vibrations can be attributed to non-covalent interactions, such as hydrophobic interactions and hydrogen bonding between the protein and polysaccharide molecules (Huang et al., 2021). The increase in hydrophobic associations in hydrogels, facilitated by non-covalent

interactions between polysaccharides and proteins, significantly influences the interfacial behavior and stability of the gelling networking system, resulting in increased mechanical strength (Abdurrahmanoglu et al., 2009; Ghosh and Bandyopadhyay, 2012). In an aqueous environment, non-polar amino acid side chains tend to aggregate to minimize contact with polar solvents (Dyson et al., 2006). Thus, hydrophobic interactions can occur between the non-polar residues of pea protein isolates and the hydrophobic pockets on the surface of the agarose. Owing to such interactions, stable complexes are formed. Pea proteins have higher levels of hydrophobic amino acids, such as leucine, valine, and isoleucine, than soy proteins (Claessens et al., 2008; Liu et al., 2019). The significant difference in the vibration intensity between pea protein and soy protein at 2,969 cm^{-1} and 1,073 cm^{-1} may be due to hydrophobic interactions between amino acids and polysaccharides in the hydrogels. However, the hydrogel structure must be analyzed using NMR to obtain a more definite conclusion.

We investigated the physical properties of the scaffolds. The scaffold should possess high water-holding capacity, porous structure, and good mechanical strength (Seah et al., 2022). Based on our results, the water absorption capacity of the soy protein scaffolds (SA and SAP) was higher than that of the pea protein scaffolds (PA and PAP), despite their similar pore sizes. The porosity of hydrogels is affected by the molecular weight of the proteins (Schmidt et al., 2008). Typically, high molecular weight proteins form larger pores in hydrogels (Guo et al., 2021). Soy and pea proteins have average molecular weights that are similar (approximately 300–600 kDa and ~380 kDa, respectively; Barac et al., 2010; Sun, 2005). Therefore, soy and pea protein scaffolds displayed similar levels of porosity. However, pea protein contains a relatively high proportion of hydrophobic amino acids, such as leucine and valine, which can reduce the overall hydrophilicity of the protein. Thus, the difference in amino acid profiles resulted in pea protein scaffolds with a lower water absorption capacity. Additionally, the compressive strength of the agarose scaffolds (SA and PA) was approximately twice that of the agar powder scaffolds (SAP and PAP), which is consistent with the FT-IR results, indicating that agarose with higher purity exhibits greater strength owing to more chemical bonds.

The cytotoxicity of the protein-polysaccharide hydrogel was assessed using the liquid extract of the scaffold, in accordance with ISO 10993-5, which is a standard method for evaluating the biocompatibility of materials intended for use in the human body (Lagonegro et al., 2017; Luo et al., 2016). In this study, ADSCs derived from Berkshire pigs were exposed to the liquid extract of the scaffold for 1 day and 3 days, and cell viability, LDH release, and live/dead staining were used to evaluate the cytotoxicity. No significant difference in cell viability or LDH release was found between the ADSCs treated with the liquid extract of the scaffold and the control group at both time points. Moreover, live/dead staining revealed no significant difference in the number of dead cells between the ADSCs treated with the liquid extracts of the scaffold and the control group on days 1 and 3. Although some dead cells were observed in ADSCs treated with PA and PAP extracts, no significant difference was found relative to the other groups. Our findings suggest that the protein-polysaccharide scaffolds used in this study are nontoxic and safe for application in cultured meat production.

Three methods, FE-SEM, counting cell in media, and DAPI staining, were employed to assess the characteristic of cell adhesion to scaffold. Our data showed that the ability of the scaffold to support cell adhesion varied significantly. In particular, the number of cells attached to SA and SAP was notably higher than that attached to PA and PAP until day 3. However, when SA and SAP were compared on day 5, SA showed a higher proliferation rate than SAP. The soy protein scaffolds displayed superior cell adhesion ability, as the number of ADSCs in the culture media with the scaffolds was lower. DAPI staining revealed that SA had a higher confluence than SAP, PA, and PAP on days 3 and 5, indicating its better proliferation ability. Agarose and agar exhibited distinct characteristics regarding cell proliferation. Agar contains impurities, such as agaropectin, which can complicate interactions with cells, potentially hindering cell growth and proliferation

(Armisén and Gaiatas, 2009). This is why scaffold-attached cells were notably higher on day 5 in the SA group compared to the SAP group.

Cell adhesion is a critical factor in scaffold-based cultured meat production and is primarily influenced by the RGD motif, which is an integrin-binding domain found in ECM proteins, such as fibronectin, fibrinogen, and vitronectin (Arnaout et al., 2005). Integrins are transmembrane proteins that combine to form a heterodimeric complex with two subunits, α and β (van der Flier and Sonnenberg, 2001). When integrin binds to an RGD-containing protein, the RGD motif binds to the integrin-binding site, leading to a conformational change in integrin and activation of intracellular signaling pathways that regulate cell adhesion, migration, proliferation, and differentiation (Hersel et al., 2003). Previous studies showed that soy protein contains the RGD sequence, as demonstrated by the soybean-derived peptide, lunasin, which contains the RGD sequence and promotes cell adhesion (Dia and de Mejia, 2011). Our findings suggest that soy protein scaffolds generally exhibited higher cell attachment ability compared to pea protein scaffolds, potentially attributed to the presence of the RGD sequence. Additionally, agarose demonstrated greater favorability for cell adherence on the scaffolds. However, it is important to acknowledge the limitations of our experiment, notably that only floating cells were counted while plate well-adhered cells were not included in the analysis. Despite this limitation, the floating cells can still serve as a proxy for assessing scaffold adhesion efficiency, as there should be a consistent ratio between plate well-attached and unattached cells across all groups.

Conclusion

In conclusion, the present study aimed to compare soy and pea proteins in developing protein-polysaccharide hydrogel scaffolds, and to evaluate their suitability for cultured meat production. The scaffolds had a porous structure, high water absorption ability, and adequate compressive strength. Cytotoxicity testing of the scaffold liquid extract revealed no significant toxicity in ADSCs. Soy protein scaffold exhibited better cell adhesion properties than the pea protein scaffold. Overall, our data suggests an economical and eco-friendly scaffold for cultured meat production, with a particular emphasis on utilizing soy proteins.

Conflicts of Interest

The authors declare no potential conflicts of interest.

Acknowledgements

This study was funded by Korea Institute of Planning and Evaluation for Technology in Food, Agriculture and Forestry (IPET) through High Value-added Food Technology Development Program, funded by Ministry of Agriculture, Food and Rural Affairs (MAFRA) (32200605CG000). The funder played no role in study design, data collection, analysis and interpretation of data, or the writing of this manuscript.

Author Contributions

Conceptualization: Kim DH, Han Seo Gu, Han Sung Gu. Investigation: Kim DH, Han Seo Gu, Lim SJ, Hong SJ, Kwon HC, Jung HS. Writing - original draft: Kim DH, Han Seo Gu. Writing - review & editing: Kim DH, Han Seo Gu, Lim SJ,

Hong SJ, Kwon HC, Jung HS, Han Sung Gu.

Ethics Approval

This article does not require IRB/IACUC approval because there are no human and animal participants.

References

Abdurrahmanoglu S, Can V, Okay O. 2009. Design of high-toughness polyacrylamide hydrogels by hydrophobic modification. Polymer 50:5449-5455.

Amitai G, Shemesh A, Sitbon E, Shklar M, Netanely D, Venger I, Pietrokovski S. 2004. Network analysis of protein structures identifies functional residues. J Mol Biol 344:1135-1146.

Armisén R, Gaiatas F. 2009. Agar. In Handbook of hydrocolloids. 2nd ed. Phillips GO, Williams PA (ed). Woodhead, Cambridge, UK. pp 82-107.

Arnaout MA, Mahalingam B, Xiong JP. 2005. Integrin structure, allostery, and bidirectional signaling. Annu Rev Cell Dev Biol 21:381-410.

Barac M, Cabrilo S, Pesic M, Stanojevic S, Zilic S, Macej O, Ristic N. 2010. Profile and functional properties of seed proteins from six pea (*Pisum sativum*) genotypes. Int J Mol Sci 11:4973-4990.

Bektas EI, Pekozer GG, Kök FN, Kose GT. 2021. Evaluation of natural gum-based cryogels for soft tissue engineering. Carbohydr Polym 271:118407.

Ben-Arye T, Shandalov Y, Ben-Shaul S, Landau S, Zagury Y, Ianovici I, Lavon N, Levenberg S. 2020. Textured soy protein scaffolds enable the generation of three-dimensional bovine skeletal muscle tissue for cell-based meat. Nat Food 1:210-220.

Benjaminson MA, Gilchriest JA, Lorenz M. 2002. *In vitro* edible muscle protein production system (mpps): Stage 1, fish. Acta Astronaut 51:879-889.

Bhat ZF, Fayaz H. 2011. Prospectus of cultured meat: Advancing meat alternatives. J Food Sci Technol 48:125-140.

Cesur S, Ulag S, Ozak L, Gumussoy A, Arslan S, Yilmaz BK, Ekren N, Agirbasli M, Kalaskar DM, Gunduz O. 2020. Production and characterization of elastomeric cardiac tissue-like patches for myocardial tissue engineering. Polym Test 90:106613.

Chen L, Guttieres D, Koenigsberg A, Barone PW, Sinskey AJ, Springs SL. 2022. Large-scale cultured meat production: Trends, challenges and promising biomanufacturing technologies. Biomaterials 280:121274.

Claessens M, Saris WHM, van Baak MA. 2008. Glucagon and insulin responses after ingestion of different amounts of intact and hydrolysed proteins. Br J Nutr 100:61-69.

Datar I, Betti M. 2010. Possibilities for an *in vitro* meat production system. Innov Food Sci Emerg Technol 11:13-22.

de Oliveira ACS, Ugucioni JC, da Rocha RA, Borges SV. 2019. Development of whey protein isolate/polyaniline smart packaging: Morphological, structural, thermal, and electrical properties. J Appl Polym Sci 136:47316.

Dia VP, de Mejia EG. 2011. Lunasin induces apoptosis and modifies the expression of genes associated with extracellular matrix and cell adhesion in human metastatic colon cancer cells. Mol Nutr Food Res 55:623-634.

Dyson HJ, Wright PE, Scheraga HA. 2006. The role of hydrophobic interactions in initiation and propagation of protein folding. Proc Natl Acad Sci 103:13057-13061.

EFSA Panel on Food Additives and Nutrient Sources added to Food. 2016. Scientific opinion on the re-evaluation of agra (E 406) as a food additive. EFSA J 14:4645.

Garrido T, Etxabide A, Guerrero P, de la Caba K. 2016. Characterization of agar/soy protein biocomposite films: Effect of agar on the extruded pellets and compression moulded films. Carbohydr Polym 151:408-416.

Ghosh AK, Bandyopadhyay P. 2012. Polysaccharide-protein interactions and their relevance in food colloids. In The complex world of polysaccharides. Karunaratne DN (ed). IntechOpen, Rijeka, Croatia. pp 395-408.

Gonzalez de Mejia E, Wang W, Dia VP. 2010. Lunasin, with an arginine–glycine–aspartic acid motif, causes apoptosis to l1210 leukemia cells by activation of caspase-3. Mol Nutr Food Res 54:406-414.

Guo L, Chai Y, Zhou F, Wang P. 2021. Preparation and properties of hyaluronic acid hydrogel modified by l-cysteine hydrochloride. IOP Conf Ser: Earth and Environ Sci 651:042022.

Habermann SM, Murphy KP. 1996. Energetics of hydrogen bonding in proteins: A model compound study. Protein Sci 5:1229-1239.

Hersel U, Dahmen C, Kessler H. 2003. RGD modified polymers: Biomaterials for stimulated cell adhesion and beyond. Biomaterials 24:4385-4415.

Hong TK, Shin DM, Choi J, Do JT, Han SG. 2021. Current issues and technical advances in cultured meat production: A review. Food Sci Anim Resour 41:355-372.

Hu J, Zhao T, Li S, Wang Z, Wen C, Wang H, Yu C, Ji C. 2019. Stability, microstructure, and digestibility of whey protein isolate: *Tremella fuciformis* polysaccharide complexes. Food Hydrocoll 89:379-385.

Huang H, Belwal T, Lin X, Limwachiranon J, Zou L, Luo Z. 2021. Novel bind-then-release model based on fluorescence spectroscopy analysis with molecular docking simulation: New insights to zero-order release of arbutin and coumaric acid. Food Hydrocoll 112:106356.

Jackson M, Mantsch HH. 1992. Halogenated alcohols as solvents for proteins: FTIR spectroscopic studies. Biochim Biophys Acta Protein Struct Mol Enzymol 1118:139-143.

Jahangirian H, Azizi S, Rafiee-Moghaddam R, Baratvand B, Webster TJ. 2019. Status of plant protein-based green scaffolds for regenerative medicine applications. Biomolecules 9:619.

Jairath G, Mal G, Gopinath D, Singh B. 2021. A holistic approach to access the viability of cultured meat: A review. Trends Food Sci Technol 110:700-710.

Lagonegro P, Rossi F, Galli C, Smerieri A, Alinovi R, Pinelli S, Rimoldi T, Attolini G, Macaluso G, Macaluso C, Saddow SE, Salviati G. 2017. A cytotoxicity study of silicon oxycarbide nanowires as cell scaffold for biomedical applications. Mater Sci Eng C 73:465-471.

Lam ACY, Can Karaca A, Tyler RT, Nickerson MT. 2018. Pea protein isolates: Structure, extraction, and functionality. Food Rev Int 34:126-147.

Langyan S, Yadava P, Khan FN, Dar ZA, Singh R, Kumar A. 2022. Sustaining protein nutrition through plant-based foods. Front Nutr 8:772573.

Las Heras K, Santos-Vizcaino E, Garrido T, Gutierrez FB, Aguirre JJ, de la Caba K, Guerrero P, Igartua M, Hernandez RM. 2020. Soy protein and chitin sponge-like scaffolds: From natural by-products to cell delivery systems for biomedical applications. Green Chem 22:3445-3460.

Lee A, Hudson AR, Shiwarski DJ, Tashman JW, Hinton TJ, Yerneni S, Bliley JM, Campbell PG, Feinberg AW. 2019. 3D bioprinting of collagen to rebuild components of the human heart. Science 365:482-487.

Lei Y, Zhao X, Li D, Wang L, Wang Y. 2022. Effects of κ-carrageenan and guar gum on the rheological properties and microstructure of phycocyanin gel. Foods 11:734.

Levato R, Jungst T, Scheuring RG, Blunk T, Groll J, Malda J. 2020. From shape to function: The next step in bioprinting. Adv Mater 32:1906423.

Lin HH, Hsieh FY, Tseng CS, Hsu S. 2016. Preparation and characterization of a biodegradable polyurethane hydrogel and the hybrid gel with soy protein for 3D cell-laden bioprinting. J Mater Chem B 4:6694-6705.

Liu J, Klebach M, Visser M, Hofman Z. 2019. Amino acid availability of a dairy and vegetable protein blend compared to single casein, whey, soy, and pea proteins: A double-blind, cross-over trial. Nutrients 11:2613.

Liu N, Wang G, Zhen Y, Shang Y, Nie F, Zhu L, Zhao Z, An Y. 2022. Factors influencing myogenic differentiation of adipose-derived stem cells and their application in muscle regeneration. Chin J Plast Reconstr Surg 4:126-132.

Louche A, Salcedo SP, Bigot S. 2017. Protein–protein interactions: Pull-down assays. In Bacterial protein secretion systems: Methods and protocols. Journet L, Cascales E (ed). Humana Press, New York, NY, USA. pp 247-255.

Luo Y, Dolder CK, Walker JM, Mishra R, Dean D, Becker ML. 2016. Synthesis and biological evaluation of well-defined poly (propylene fumarate) oligomers and their use in 3D printed scaffolds. Biomacromolecules 17:690-697.

Mobaraki M, Ghaffari M, Yazdanpanah A, Luo Y, Mills DK. 2020. Bioinks and bioprinting: A focused review. Bioprinting 18:e00080.

O'brien FJ. 2011. Biomaterials & scaffolds for tissue engineering. Mater Today 14:88-95.

Pan H, Pei F, Ma G, Ma N, Zhong L, Zhao L, Hu Q. 2022. 3D printing properties of *Flammulina velutipes* polysaccharide-soy protein complex hydrogels. J Food Eng 334:111170.

Ran X, Lou X, Zheng H, Gu Q, Yang H. 2022. Improving the texture and rheological qualities of a plant-based fishball analogue by using konjac glucomannan to enhance crosslinks with soy protein. Innov Food Sci Emerg Technol 75:102910.

Reddy N, Jiang Q, Yang Y. 2011. Novel wheat protein films as substrates for tissue engineering. J Biomater Sci Polym Ed 22:2063-2077.

Schmidt JJ, Rowley J, Kong HJ. 2008. Hydrogels used for cell-based drug delivery. J Biomed Mater Res A 87A:1113-1122.

Seah JSH, Singh S, Tan LP, Choudhury D. 2022. Scaffolds for the manufacture of cultured meat. Crit Rev Biotechnol 42:311-323.

Specht EA, Welch DR, Clayton EMR, Lagally CD. 2018. Opportunities for applying biomedical production and manufacturing methods to the development of the clean meat industry. Biochem Eng J 132:161-168.

Stephens N, Di Silvio L, Dunsford I, Ellis M, Glencross A, Sexton A. 2018. Bringing cultured meat to market: Technical, socio-political, and regulatory challenges in cellular agriculture. Trends Food Sci Technol 78:155-166.

Sun XS. 2005. Soy protein adhesives. In Bio-based polymers and composites. Wool RP, Sun XS (ed). Academic Press, Burlington, MA, USA. pp 327-368.

Takahashi K, Yamanaka S. 2006. Induction of pluripotent stem cells from mouse embryonic and adult fibroblast cultures by defined factors. Cell 126:663-676.

Tansaz S, Singh R, Cicha I, Boccaccini AR. 2018. Soy protein-based composite hydrogels: Physico-chemical characterization and *in vitro* cytocompatibility. Polymers 10:1159.

te Nijenhuis K. 1997. Thermoreversible networks: Viscoelastic properties and structure of gels. In Advances in polymer science. Guo M (ed). Springer, Heidelberg, Germany. pp 194-202.

Tiberius V, Borning J, Seeler S. 2019. Setting the table for meat consumers: An international delphi study on *in vitro* meat. npj Sci Food 3:10.

Tsuji W, Peter Rubin J, Marra KG. 2014. Adipose-derived stem cells: Implications in tissue regeneration. World J Stem Cells 6:312-321.

van der Flier A, Sonnenberg A. 2001. Function and interactions of integrins. Cell Tissue Res 305:285-298.

Wollschlaeger JO, Maatz R, Albrecht FB, Klatt A, Heine S, Blaeser A, Kluger PJ. 2022. Scaffolds for cultured meat on the basis of polysaccharide hydrogels enriched with plant-based proteins. Gels 8:94.

Xiang N, Yuen JSK Jr, Stout AJ, Rubio NR, Chen Y, Kaplan DL. 2022. 3D porous scaffolds from wheat glutenin for cultured meat applications. Biomaterials 285:121543.

Yan W, Zhang B, Yadav MP, Feng L, Yan J, Jia X, Yin L. 2020. Corn fiber gum-soybean protein isolate double network hydrogel as oral delivery vehicles for thermosensitive bioactive compounds. Food Hydrocoll 107:105865.

Yixue S, Bin C, Yuan G, Chaoxi W, Lingmin Z, Peng C, Xiaoying W, Shunqing T. 2013. Modification of agarose with carboxylation and grafting dopamine for promotion of its cell-adhesiveness. Carbohydr Polym 92:2245-2251.

Zhang G, Zhao X, Li X, Du G, Zhou J, Chen J. 2020. Challenges and possibilities for bio-manufacturing cultured meat. Trends Food Sci Technol 97:443-450.

Zheng YY, Chen Y, Zhu HZ, Li CB, Song WJ, Ding SJ, Zhou GH. 2022. Production of cultured meat by culturing porcine smooth muscle cells *in vitro* with food grade peanut wire-drawing protein scaffold. Food Res Int 159:111561.

Zhu P, Huang W, Guo X, Chen L. 2021. Strong and elastic pea protein hydrogels formed through pH-shifting method. Food Hydrocoll 117:106705.